SOME FACTORS AFFECTING THE REACTIVITY OF SIZED PARTICLE CARBONS TO CARBON DIOXIDE*†

By P. L. WALKER, jun. and J. R. NICHOLS

(*Fuel Technology Dept., Pennsylvania State University*)

The reactivity of fifteen coked or graphitized particle carbons (particle sizes in the range 6 to 48 mesh) derived from either petroleum or coal was investigated over the temperature range 1050–1200°. The operation was carried out under fixed-bed conditions with reactivities determined from the weight loss of the bed with time. Reactivity data were correlated with the following properties of the carbons—specific surface area, unit cell parameters, electrical resistivities, bulk densities, chemical composition, and spectrographic ash analyses, but no consistent correlations were found. The effects of changing operating conditions during reaction (gas flow rate, carbon and chip weight, carbon particle size, and temperature) were investigated to clarify the nature of the reactor.

Introduction

The widespread importance of the heterogeneous gasification reactions of carbons in present-day industry necessitates a complete understanding of the mechanism of these reactions. On the one hand, the primary interest in gasification is related to the conversion of carbonaceous materials to either gaseous fuels or synthesis gas, where of primary concern is the attainment of high gasification rates. On the other hand, the primary interest is connected with the lack of gasification of carbons and graphites when used as electrodes, structural carbons or moderators in atomic reactors. In either case, a basic understanding of the relationship between reactivity of carbon to gases and the physical properties of the carbons is essential.

Considerable effort has been expended in an attempt to understand completely the physical structure of carbon bodies which consist of a filler material (petroleum coke, coal coke, anthracite coal, or carbon black) and a binder (coal-tar or petroleum pitch) and to relate the physical properties to the reactivity of the carbon bodies with carbon dioxide.[1-13] Unfortunately, interpretation of reactivity results for carbon bodies which are composed of two different raw materials is difficult because of the inherent difference in reactivity of each raw material, the lack of micro-homogeneity in the sample because of difference in location of the filler and binder in the body, and the interaction of the filler and binder phases during processing, which alters the properties of both materials. Furthermore, fabrication of carbon bodies by extrusion or moulding produces considerable orientation of the basal plane structure, which results in anisotropic properties for the body. Reactivity of the body to gases is found to be one of the properties most highly affected by orientation of the basal plane structure, since this orientation determines the fraction of basal plane carbon atoms in the surface of the body—the higher the fraction the lower the reactivity of the carbon, all other things equal.

To obtain information on the relative reactivities of typical filler and binder materials, which are used in the manufacture of carbon bodies, a carbon particle reactor has been designed and employed in this work. The effect on their reactivity of grinding carbon bodies to known particle size has also been studied with the new reactor. As in previous work, reactivities of the carbons to carbon dioxide have been correlated with different physical properties of the carbons, such as surface area, electrical resistivity, crystallographic parameters, impurity content, and chemical composition.

In addition to the wish to compare reactivities of different carbons in the reactor, it was desired to characterize the nature of the reactor itself. Therefore, the effects of varying the weight of carbon, the weight of chips supporting the carbon, the particle size of carbon and chips, the gas flow rate, and the reaction temperature on gasification rate were also investigated for several carbons.

Experimental

Reaction-rate apparatus.—The reaction-rate apparatus, Fig. 1, has been described in considerable detail in a previous publication.[1] Briefly, a furnace containing copper oxide operating at 450° is used to remove traces of hydrogen from the helium employed as the preheating medium. The flow rates of all gases are determined by rotameters. Traces of oxygen are removed from the helium and carbon dioxide streams by passage over copper wool at 650°. The gases then pass through an activated-alumina tower to remove traces of water, and then

through a preheater operating at 850° and into the reaction-rate furnace, which is a Burrell Model A1-13 Globar tube furnace turned on end. Running through the furnace is a high-temperature porcelain combustion tube approximately 34 in. long and 1⅛ in. i. d. Concentric with the combustion tube is a ½-in. porcelain tube reaching just into the hot part of the furnace and serving as a pier upon which the sample rests during the reaction. The space between the tubes is filled with 6 × 8-mesh porcelain chips.
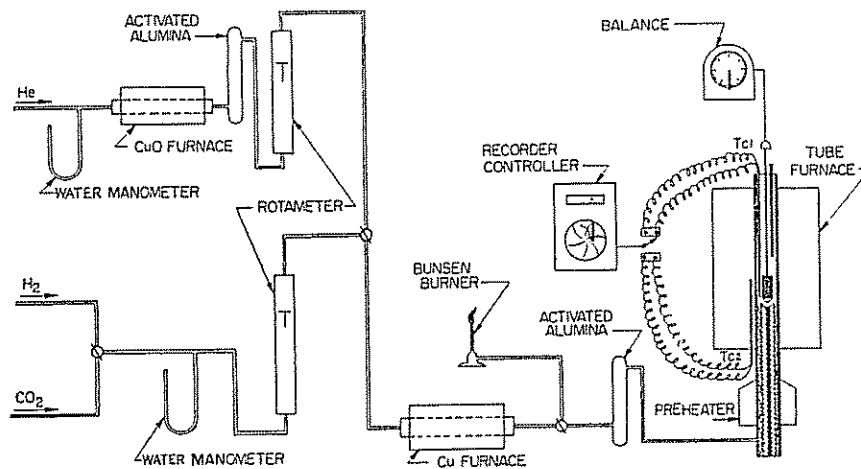

FIG. 1. *Reaction-rate apparatus*

In the present investigation, the sample is held in a special reactor shown in Fig. 2. The crucible is approximately 2 in. high by ¾-in. in diameter, with wall thickness about 1/16-in. It has 16 1/16-in. holes in the bottom, equally spaced in two rings of eight with a ⅛-in. hole in the centre to admit the support rod. The support rod is a ⅛-in. porcelain rod with a double cone of maximum diameter of ½-in. cast on one end. The cover of the crucible has four 1/16-in. holes equally spaced in a ring around a ⅛-in. hole through which passes the support rod. The cover fits inside the crucible and flush with the top edge, being supported by four projecting lugs cast into the sides of the crucible. At the top of the support rod, a hanger is attached, by means of which the sample holder assembly is suspended from a Roller–Smith torsion balance, which weighs to an accuracy of about ± 20 mg.
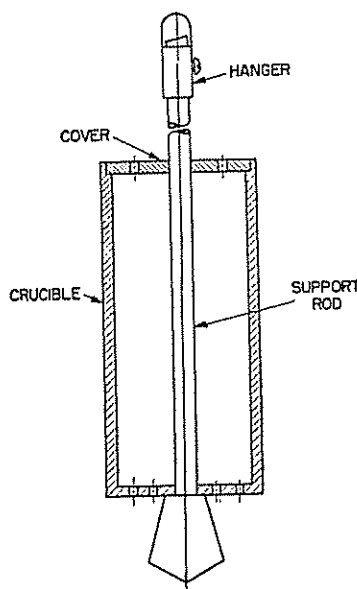

FIG. 2. *Carbon particle reactor*

In brief, the procedure for making a run is first to reduce the copper wool with hydrogen and to flush briefly with carbon dioxide and then with helium, all being sent out through the burner. Next, helium is admitted to the furnace for a purge of about 30 min. The sample is prepared for the run as in the following typical sequence: taring the crucible, adding 6 × 8-mesh (Tyler Standard Series) porcelain chips (about 2 g.) until light is not visible through the bottom, adding 8 × 20-mesh chips until the total chip weight is about 6 g., adding the pre-weighed sample and assembling the whole sample holder. For small mesh sizes, the support rod must be inserted before the sample is added and the whole assembly gently bounced on the bench top several times to settle the sample and to ensure that none will fall out the bottom. With the sample ready and the furnace purged, the next step is to remove the upper thermocouple and combustion tube cover (provision is made to control temperature from another thermocouple, Tc2 in Fig. 1, during this period) and to lower the sample assembly slowly into the furance (usually taking about 5 to 7 min.). A preheat period of about an hour is begun when the sample is in the furnace and the upper thermocouple is again controlling. Sample weight is recorded at this time.

The actual rate determination is begun with a 2-min. stream of carbon dioxide at a high flow rate to flush out the helium. Then, over a subsequent ½-min. period before the so-called zero time, the flow rate is adjusted to the operating condition and the sample is brought almost to balance, preparatory to weighing at zero time. Time, sample weight, gas-flow rate, and temperature are then recorded at definite time intervals until the desired weight loss has been reached. In the present investigation, this weight loss is taken as the place where reaction rate begins to taper off. After achieving the desired weight loss, helium is again turned on; and the sample is slowly removed from the furnace. After cooling, the residue is weighed and a material balance is struck as a check.

Apparatus used for analysis

Low-temperature gas-adsorption apparatus.—A standard gas-adsorption apparatus was employed to determine the surface area of the carbons (6 × 8 mesh) and has been described recently.[1] Surface areas were determined from krypton adsorption at liquid-nitrogen temperatures using the BET equation.[14] Krypton was used as the adsorbate instead of nitrogen, as in the usual case, because of the low specific surface areas of the carbons investigated. A paper by Beebe and co-workers[15] discusses the virtues of using krypton adsorption for low-area samples.

X-ray diffraction apparatus.—A 164° (2θ) General Electric X-ray diffraction unit, XRD-3, with copper radiation was used to determine interlayer spacings and crystallite sizes for the carbon samples, as previously discussed.[4]

Electrical resistivity apparatus.—The apparatus and the procedure employed has been recently described.[16]

Spectrographic ash analysis apparatus.—Exposures were made on glass photographic plates using a Jarrell-Ash 21-foot grating spectrograph. Some 35 elements were sought qualitatively. Subsequently, the most prominent elements were determined quantitatively by measuring the density of the proper lines between per cent transmissions of 3 and 40, using either an ARL Comparator Densitometer or a Hilger Microphotometer. These readings were plotted as optical density against exposure in the constant-slope portion of an H and D curve.[17] From these plots, the percentage of the total sample as the element under consideration is calculated by comparison with a known standard on each plate.

Chemical analysis apparatus.—Chemical analyses were carried out according to the A.S.T.M. standard procedures for coal and carbon.[18, 19]

Description of reactants

Reactants may be divided into two major groups, solid and gaseous, with the former divided into three sub-groups: foundry or cupola fuels, electrode raw materials, and crushed electrodes.

Solid reactants

Foundry or cupola fuels.—SSC-Semet Solvay coke is a standard high-grade, low-temperature, by-product foundry coke, produced at ∼ 580° and probably from a mixture of 65% high-volatile and 35% low-volatile bituminous coal.

HCC is a so-called high-carbon coke composed of 5–25% petroleum coke and/or anthracite coal screened to 60% —⅛-in., mixed with high-volatile bituminous coal, and carbonized at ∼ 1000°.

Electrode raw materials.—950 PC and 2750 PC are petroleum cokes heat-treated, respectively, at 950° and 2750°.

950 PPC and 2750 PPC are formed by carbonization of petroleum pitch to give petroleum pitch cokes subsequently heat-treated at 950° and 2750°, respectively, as with the petroleum cokes above.

950 CTPC and 2750 CTPC are formed by carbonization of coal-tar pitch and the coal-tar pitch coke is subsequently heat-treated at 950° and 2750°.

Crushed electrodes.—950 GBC 'A' and 950 GBC 'C' are typical standard-grade amorphous carbon electrodes from two manufacturers. Specific conditions of manufacture are not known, but a typical procedure is approximately as follows: a mixture of about 25% of coal-tar pitch as binder and 75% of calcined petroleum coke flour (60% through 200 mesh) as filler material is prepared. The mixture is heated, well blended, and finally extruded into ⅝-in.-diameter rods. These rods, after cooling and curing, are gas-baked at about 950° for several weeks.

950 *GBC ' B '* is another gas-baked amorphous carbon electrode, which differs only in that the raw filler material is about 87% of 950 GBC ' A ' and 13% of material similar to 2750 GC ' B ' described below.

950 *LB* is also a gas-baked carbon electrode prepared as previously described, with lampblack substituted for petroleum coke as the filler material.

2750 *GC ' A '* and 2750 *GC ' B '* are two graphitized carbon electrodes from the same. manufacturer but from different lots and in different extrusion sizes. Preparation is about the same as for amorphous carbons up through the gas-baking step, except that ' A ' is extruded in ½-in. diameter while ' B ' is in the normal ⅝-in. size. After gas-baking, graphitization is performed.

3000 *Spec*—careful selection of raw materials and graphitizing at 3000° gives this special spectroscopic grade graphite, apparently the best artificial graphite commercially available.

Gaseous reactants

Carbon dioxide.—The carbon dioxide is of the highest purity obtainable commercially, listed at 99·956% purity, the 0·044% impurity being water vapour.

Helium.—Although helium is not strictly a reactant, high purity is none the less essential for the well-being of the reaction rate determination; and gas of the highest commercial purity is again employed, this being listed at 99·8% purity, the 0·2% impurity being mostly nitrogen.

Results

Physical and chemical properties of the untreated carbons

The physical and chemical properties of the carbons determined during this investigation are listed in Tables I–V. Table I gives the specific surface areas of the various particulate carbons, as determined by krypton adsorption. The areas are low as previously mentioned; lampblack has a somewhat higher area because of its smaller particle size. Change in area with heat-treatment temperature is available for the two pitch cokes. Heat treatment is seen to increase the area in both cases. The results for the petroleum pitch coke are commonly observed for carbonaceous materials.[20]

Table I

Surface areas of carbons

Sample	Area, m^2/g.	Sample	Area, m^2/g.
SSC	0·16	2750 CTPC	0·23
HCC	0·53	950 GBC ' A '	0·51
950 PC	0·37	950 GBC ' B '	1·02
2750 PC	0·48	950 GBC ' C '	0·29
950 PPC	0·42	950 LB	3·06
950 PPC*	0·86	2750 GC ' A '	0·91
2750 PPC	0·45	2750 GC ' B '	1·45
950 CTPC	0·08	3000 Spec	0·67
950 CTPC†	0·13		

*950 PPC heated to 1100° in helium.
†950 CTPC heated to 1100° in helium.

Heating to temperatures between 1000 and 1300° removes most of the hydrogen and oxides of carbon from the material producing surface roughness and an accompanying increase in surface area. Heating to higher temperatures produces crystallite growth and orientation, resulting in some decrease in surface roughness and internal particle porosity, with an accompanying surface area decrease. The area results for the coal-tar pitch coke suggest that the maximum surface area for this sample is reached at a temperature somewhat in excess of 1100°.

In Table II, *X*-ray crystallographic data for the carbons are presented. Reproducibility (3 slides of each sample) is better than ±10% for crystallite size and for most d-spacing

Table II

Crystallite sizes and d-spacings of carbons

Sample	L_a, Å	L_c, Å	d-Spacing, Å	Sample	$\overline{L_a}$, Å	$\overline{L_o}$, Å	d-Spacing, Å
SSC	—	15	3·48 ± 0·01	2750 CTPC	330	235	3·3662 ± 0·0001
HCC	51	18	3·50 ± 0·01	950 GBC 'A'	55	33	3·461 ± 0·009
950 PC	—	22	3·47 ± 0·02	950 GBC 'C'	62	41	3·450 ± 0·005
2750 PC	650	510	3·3610 ± 0·0002	950 LB	59	28	3·484 ± 0·005
950 PPC	31	14	3·627 ± 0·008	2750 GC 'A'	720	990	3·3589 ± 0·0008
2750 PPC	880	385	3·3586 ± 0·0005	2750 GC 'B'	∞	900	3·3596 ± 0·0003
950 CTPC	37	13	3·644 ± 0·007	3000 Spec	∞	∞	3·3576 ± 0·0004

(No tests made on sample 950 GBC ' B '.)

determinations. It is to be noted that reproducibility of the d-spacing data improves the more graphitic the material is, as is to be expected. Average crystallite diameter values for the SSC and 950 PC samples are not reported because of the weakness of their (10) diffraction peak. No information is presented for 950 GBC ' B ', since this sample is a mixture of amorphous and graphitic material and, therefore, shows distorted X-ray peaks.[4] For several samples, the diffraction line width was so small that the major contribution of instrumental broadening could not be satisfactorily removed, and, therefore, the crystallite sizes are reported as effectively infinity.

Table III presents electrical resistivity and bulk density data as a function of pressure applied to the various –200 mesh samples. The especially high electrical resistivity of the unreacted, raw SSC, along with the major change on heating in helium to 1100°, is in accord with the known marked change[21] of resistivity in the temperature range between the formation of this coke ($\sim$ 580°) and 1100°. As expected, the samples heated to graphitization temperatures show a lower electrical resistivity and higher bulk density than the gas-baked and coked materials. The bulk densities of the graphitized samples are found to increase more rapidly with increasing pressure than their amorphous carbon counterparts, probably because of the greater ease of particle–particle slippage in the graphitized samples. The extent of change in electrical resistivity with pressure can be attributed to both the extent of change in bulk density (more area of particle–particle contact) and differences in the amount of oxygen on the carbon surface.[16] The greater the increase in bulk density and the higher amount of surface oxygen complex, the greater is the expected change in resistivity with change in pressure. For several samples, resistivities were determined after extensive burn-off at $\sim$ 1100°. It is seen that despite the burn-off which would decrease the bulk density of the sample and increase resistivity, the resistivity is decreased below that of the raw material because of the strong effect which volatile matter release in this temperature range has on decreasing the resistivity.[21]

Table III

Resistivities and bulk densities of carbon

Sample	Resistivity, ohm-cm.³/cm., at			Bulk density, g./c.c., at		
	2500 p.s.i.	5000 p.s.i.	10,000 p.s.i.	2500 p.s.i.	5000 p.s.i.	10,000 p.s.i.
SSC	197·6	94·2	52·0	1·11	1·16	1·30
SSC†	0·0571	0·0341	0·0225	1·28	1·37	1·52
SSC‡	0·0443	0·0283	0·0177	1·33	1·42	1·53
HCC	0·0523	0·0315	0·0201	1·39	1·44	1·56
950 PC	0·0272	0·0180	0·0120	1·45	1·57	1·63
2750 PC	0·0143	0·0098	0·0076	1·51	1·64	1·88
950 PPC	0·1345	0·0804	0·0519	1·25	1·33	1·40
2750 PPC	0·0094	0·0076	0·0054	1·60	1·87	2·01
950 CTPC	0·2706	0·1581	0·1022	1·27	1·32	1·44
2750 CTPC	0·0102	0·0073	0·0047	1·54	1·66	1·90
950 GBC ' A '	0·0403	0·0270	0·0173	1·28	1·40	1·53
950 GBC ' B '	0·0151	0·0106	0·0078	1·42	1·53	1·70
950 GBC ' B '*	0·0085	0·0065	0·0053	1·47	1·65	1·93
950 GBC ' C '	0·0260	0·0177	0·0112	1·29	1·40	1·53
950 LB ··	0·0344	0·0223	0·0148	1·07	1·15	1·26
2750 GC ' A '	0·0063	0·0059	0·0033	1·61	1·75	1·96
2750 GC ' B '	0·0097	0·0052	0·0033	1·54	1·74	1·91
3000 Spec	0·0098	0·0067	0·0045	1·83	1·87	1·96

†Reacted to 52% weight loss at 1115°.
‡Heated at 1115° in helium for 3 h.
*Reacted to about 70% weight loss at 1100°.

Table IV presents the chemical analyses for the various carbons. The combined percentage of oxygen, nitrogen, and sulphur is reported by difference. These data are as expected; the ash content decreases and the carbon content increases on graphitization.

Table V presents the spectrographic ash analyses for the carbons. All samples were run in duplicate and were repeated again if agreement was not within ±10%. Most values, however, agreed to within 1%.

Reactivity of the carbons

Table VI presents the reactivity data for the carbons at 1100°. Two runs were made on each carbon and the average value with plus and minus variations reported. Figs. 3 & 4 present several, selected, experimental curves of weight loss as a function of time. These curves are

Table IV

Chemical analyses of carbons

Sample	% Moisture	% Ash	% H	% C	% N + O + S
SSC*	1·53	6·83	2·37	85·00	4·27
HCC†	0·38	5·50	0·41	92·88	0·83
950 PC	0·06	0·12	0·22	97·85	1·75
2750 PC	0·02	0·01	0·19	99·57	0·21
950 PPC	0·26	0·65	1·13	96·99	0·97
2750 PPC	0·04	0·04	0·12	99·02	0·78
950 CTPC	0·60	0·33	1·27	95·68	2·12
2750 CTPC	0·06	0·26	0·21	99·62	—
950 GBC ' A '	0·58	0·24	0·28	97·37	1·53
950 GBC ' B '	0·05	0·58	0·13	97·61	1·63
950 GBC ' C '	0·00	0·32	0·07	98·32	1·29
950 LB	0·05	0·22	0·09	98·93	0·71
2750 GC ' A '	0·04	0·09	0·17	99·60	0·10
2750 GC ' B '	0·05	0·28	0·22	99·39	0·06
3000 Spec	0·02	0·02	0·11	99·78	0·07

*Volatile matter 6·75%. †Volatile matter 0·71%.

Table V

Spectrographic ash analyses (%) of carbons

Sample	SiO₂	Fe₂O₃	Al₂O₃	MgO	CaO	CuO	TiO₂	V₂O	MnO
SSC	0·95	0·410	0·660	0·020	0·046	0·015	0·182	0·008*	0·004*
HCC	0·95	0·325	0·530	0·021	0·111	0·014	0·162	0·008*	0·004*
950 PC	0·018	0·024	0·024	0·005	0·010	0·002	ND	0·01*	ND
275 0 PC	0·014	0·019	0·014	0·002	ND	0·002	ND	0·001*	ND
9500PPC	0·106	0·054	0·140	0·006	0·017	0·006	0·009	0·001*	0·003*
2750 PPC	0·012	0·048	0·012	0·0009	ND	0·002	ND	ND	ND
950 CTPC	0·077	0·086	0·076	0·005	0·018	0·009	0·012	ND	0·004*
2750 CTPC	0·017	0·073	0·011	0·0009	0·006	0·002	0·010	0·002*	ND
950 GBC ' A '	0·032	0·054	0·068	0·008	0·009	0·004	TR	0·038	0·005
950 GBC ' B '	0·088	0·124	0·068	0·007	0·006	0·004	TR	0·005	0·005
950 GBC ' C '	0·051	0·052	0·053	0·007	0·009	0·005	TR	0·038	0·005
950 LB	0·044	0·066	0·039	0·003	0·006	0·004	TR	0·030	0·005
2750 GC ' A '	0·020	0·015	0·022	0·001	0·009	0·003	0·022	0·002*	0·000X
2750 GC ' B '	0·022	0·005*	0·005	0·0006	0·008	0·004	0·018	ND	ND

3000 Spec Ash is almost non-existent, but what there is consists of a trace of iron and magnesium and possible traces of sodium and copper, with no other elements detected.

Ag: in 950 CTPC, 2750 CTPC, and 950 PPC = 0·001*; ND in all the rest.
B: in 2750 PPC, 2750 GC ' A ', and 2750 GC ' B ' = 0·00X, and 2750 CTPC = 0·03*; ND in all the rest.
Be: trace in SSC and HCC; ND in all the rest.
Cd: may be present in trace amounts in 950 GBC ' A '; ND in all the rest.
Cr: SSC and HCC = 0·01*; 950 GBC ' A ', 950 GBC ' B ', 950 GBC ' C ', and 950 LB = TR; ND in all the rest.
K, Na: probably present in trace amounts in all samples.
Ni: all samples probably have a trace, except 950 GBC ' B ' = 0·029% and 2750 GC ' A ' and 2750 GC ' B ' = ND.
Pb: SSC and HCC = 0·01*; 950 CTPC = 0·03*; 950 GBC ' A ', 950 GBC ' B ', and 950 GBC ' C ' = 0·04*; ND in all the rest.
As, Ba, Bi, Co, Ga, Ge, Mo, P, Sb, Sn, Sr, Zn and Zr: sought but not detected.
ND = Not detected.
TR = Trace.
* = Maximum values.

Table VI

Reaction rates of various carbons at 1100°

Sample	Reaction rate, g./h.	Sample	Reaction rate, g./h.
SSC	0·22 ± 0·01	950 GBC ' A '	0·40 ± 0·01
HCC	0·25 ± 0·01	950 GBC ' B '	0·41 ± 0·05
950 PC	0·20 ± 0·00	950 GBC ' C '	0·31 ± 0·00
2750 PC	0·19 ± 0·01	950 LB	0·44 ± 0·00
950 PPC	0·04 ± 0·00	2750 GC ' A '	0·40 ± 0·00
2750 PPC	0·21 ± 0·00	2750 GC ' B '	0·20 ± 0·01
950 CTPC	0·10 ± 0·02	3000 Spec	0·05 ± 0·01
2750 CTPC	0·34 ± 0·01		

*Each rate run was carried out at the ' constant ' condition of a 2-g. sample of 6 × 8-mesh material over a 6-g. chip bed, with a gas flow rate of 2200 c.c./min. (70°F, and 14·7 p.s.i.a.) and a reaction temperature of 1100°.
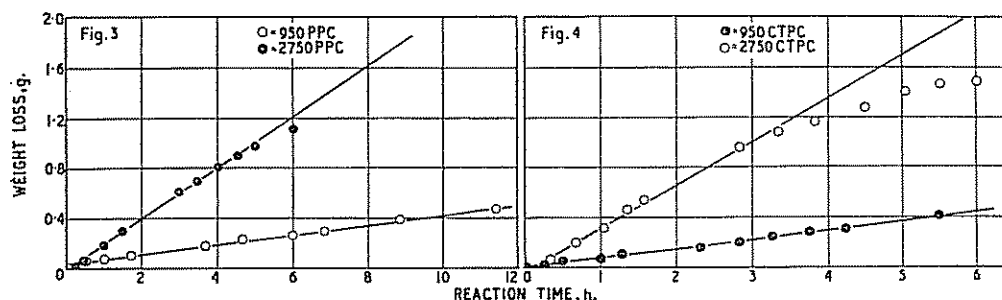
FIG. 3. *Reaction rate curves for 950 PPC and 2750 PPC at 1100°*
FIG. 4. *Reaction rate curves for 950 CTPC and 2750 CTPC at 1100°*

similar in shape to those found when reacting rod samples[1, 10]—an increasing rate during the early stages of burn-off, a region of essentially constant rate, and a region of continuously decreasing rate at higher burn-off. These regions have been qualitatively related to the change in total surface area of the sample[1, 10] on gasification.   The rates reported in Table VI represent values taken from the constant-rate portion of the curve. Of particular note in Table VI is the fact that graphitized petroleum-pitch coke and coal-tar-pitch coke reacted appreciably more rapidly than did their amorphous carbon counterparts.

A thorough investigation of the effect of changing operating variables on the reactivity results was also performed and the data are reported in Table VII. Figs. 5–10 present the reaction rate curves following the different changes in operating conditions. Doubling the chip weight or carbon dioxide flow rate has, within practical operating limits, a negligible effect on the reaction rate of 2750 GC ' B ' at ~ 1100°, while a similar increase in the weight of 950 GBC ' B ' results in a 29% increase in reaction rate at 1100°. Change in the particle size of 950 GBC ' B ' from 6 × 8-mesh to 40 × 48-mesh has a negligible effect on reaction rate.

For both 2750 GC ' B ' (6 × 8-mesh) and 950 GBC ' B ' (14 × 20-mesh) the effect of change in temperature on reactivity was investigated. Plotting the reaction rate results, expressed as weight in g. reacting per hour, on an Arrhenius plot, as previously discussed,[1, 10] activation energies of 46 and 32 kcal./mole are determined for 2750 GC ' B ' and 950 GBC ' B ', respectively.

Discussion

Before discussing the reactivity results, it is desirable to consider the significance of the calculations presented in the Appendix of this paper. At reaction conditions of 1100° and

Table VII

Effect of operating variables on reaction rates of 950 GBC ' B ' and 2750 GBC ' B '

Sample	Reaction rate, g./h.	Chip weight, g.	Flow rate*	Sample weight, g.	Mesh size	Temp., °C
2750 GC 'B '	0·22 ± 0·01	4	16	2	6 × 8	1100
2750 GC 'B '	0·20 ± 0·01	6	16	2	6 × 8	1100
2750 GC 'B '	0·20 ± 0·00	8	16	2	6 × 8	1100
2750 GC 'B '	0·28 ± 0·01	6	10	2	6 × 8	1130
2750 GC 'B '	0·30 ± 0·00	6	16	2	6 × 8	1130
2750 GC 'B '	0·30 ± 0·01	6	22	2	6 × 8	1130
950 GBC 'B '	0·41 ± 0·05	6	16	2	6 × 8	1100
950 GBC 'B '	0·47 ± 0·01	6	16	3	6 × 8	1100
950 GBC 'B '	0·53 ± 0·02	6	16	4	6 × 8	1100
950 GBC 'B '	0·41 ± 0·01	6	16	2	14 × 20	1100
950 GBC 'B '	0·40 ± 0·00	6	16	2	40 × 48	1100
950 GBC 'B '	0·25 ± 0·01	6	16	2	6 × 8	1050
950 GBC 'B '	0·25	6	16	2	14 × 20	1050
950 GBC 'B '	0·59 ± 0·02	6	16	2	14 × 20	1150
2750 GC 'B '	0·62	6	16	2	6 × 8	1200

*10 = 1450 c.c./min. (70°F and 14·7 p.s.i.a.).
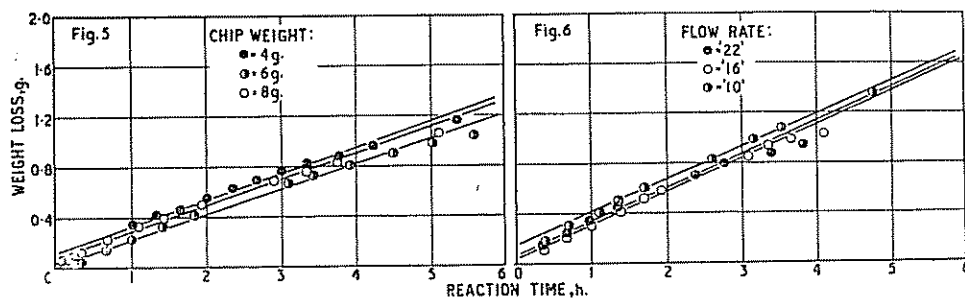16 = 2200 c.c./min.   22 = 2850 c.c./min.

FIG. 5. *Effect of variation in chip weight on reaction rate curves for 2750 GC ' B ' at 1100°*
FIG. 6. *Effect of variation in carbon dioxide flow rate on reaction rate curves for 2750 GC ' B ' at 1130°*
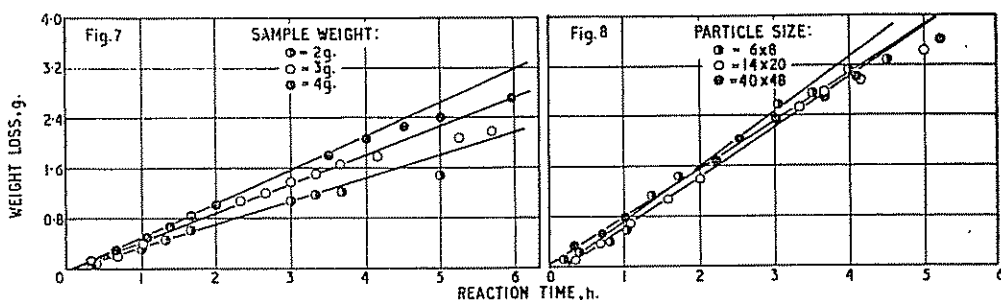

FIG. 7. *Effect of variation in weight of carbon on reaction rate curves for 950 GBC ' B ' at 1100°*
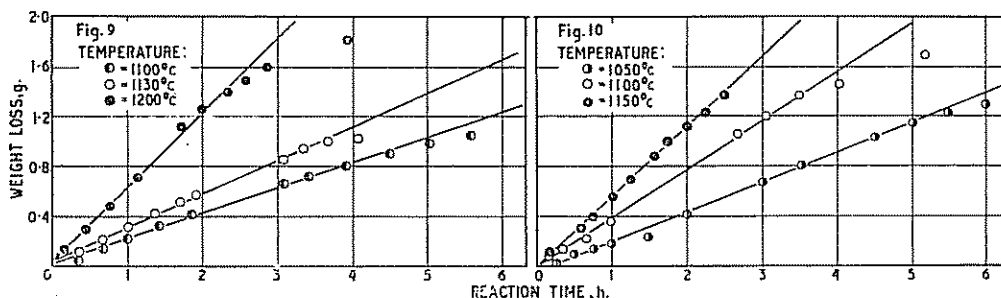FIG. 8. *Effect of variation in carbon particle size on reaction rate curves for 950 GBC ' B ' at 1100°*

FIG. 9. *Effect of temperature on reaction rate curves for 2750 GC ' B '*
FIG. 10. *Effect of temperature on reaction rate curves for 950 GBC ' B '*

atmospheric pressure, the proportion of carbon monoxide in the carbon monoxide–carbon dioxide mixture at equilibrium is 99·2%.   It is seen from Table IX that the concentrations of carbon monoxide leaving the reactor under some typical operating conditions is far removed from equilibrium.   Therefore, the reactivities measured for the carbons at 1100° are not affected by the attainment or close approach of equilibrium in the reactor.   Furthermore, the high values for the calculated activation energies (32 and 46 kcal./mole) for the reactions of 950 GBC ' B ' and 2750 GC ' B ', respectively, are a clear indication that mass transport of reactant gas between the main stream and the exterior carbon surface was not rate-controlling.[22] This is further confirmed by the negligible effect which changes in carbon dioxide flow-rate through the reactor (produced by changing the total carbon dioxide flow rate, by changing the weight of chips, or by changing the particle size of the carbon), has on the reactivity of the carbons as seen in Table VII.   Where external mass transport is reaction-rate controlling, the reactivity of the carbon is proportional to approximately the 0·45 power of gas velocity.[23]

Table VIII presents, for comparison, data on the reactivities of six carbon samples, which were previously reacted in rod form[5, 10] (½-in. diameter, 2 in. long), with the data obtained in the present work.   With the exception of 950 LB, the reaction rates are in the same relative

Table VIII

*Comparison of reactivities of particulate carbons
with their rod counterparts at 1100°*

Sample	Present specific rate*	Previous specific rate*	Present relative rate	Previous relative rate	Ratio of specific rates, previous to present
950 GBC ' A '	0·292	0·566	2·02	2·18	2·01
950 GBC ' B '	0·304	0·572	2·08	2·20	1·88
950 GBC ' C '	0·212	0·368†	1·56	1·48	1·74
950 LB	0·303	0·414	2·22	1·65	1·37
2750 GC ' B '	0·127	0·243	1·00‡	1·00‡	1·91
3000 Spec	0·029	0·051	0·25	0·22	1·76

*Specific rate, in g. per h. per g. per unit concentration of CO_2, is based on average sample weight for the constant-rate portion of the curve between 10 and 30% burn-off.

†No constant rate was reached previously, but instantaneous rate at the region where the present rate was taken is approximately this value.

‡2750 GC ' B ' was taken as the basis of the relation.

order in the two sets of experiments. Undoubtedly reduction in particle size of the carbon enhances the reactivity of 950 LB more than that of the other carbons because of the smaller average macropore size present in bodies made from lampblack than from typical petroleum cokes.[6] The smaller the pore sizes within a reacting carbon body the more effective reduction in particle size will be on increasing reactivity, as discussed by Walker & Raats.[10]

Despite the reduction in particle size for these six carbons, which would increase their specific surface area and decrease the extent of internal diffusion control, their reactivities to carbon dioxide have all decreased. It is suspected that this is a result of the inability to remove the effect of carbon monoxide on reaction rates by a simple partial pressure correction, as herein employed. Because of the much lower volume of carbon dioxide flowing past the carbon surface per unit time in this work than when rod samples were reacted, the concentration of carbon monoxide built up is considerably higher. Gadsby and co-workers[24] theorize that carbon monoxide poisons the carbon–carbon dioxide reaction by chemisorption of carbon monoxide on active sites. Ergun[25] postulates that carbon monoxide is more effective in reducing the rate of reactivity of carbon to carbon dioxide than is a diluent since it determines the percentage of carbon sites occupied by oxygen and, hence, the rate of gasification. Walker and co-workers[1] show visually the effect of carbon monoxide poisoning during the reaction of a gas-baked carbon rod with carbon dioxide by observing the strong, preferential reaction of the rod at the entering end of the furnace.

Further evidence (Table VII) that the inhibiting effect of carbon monoxide on the carbon reaction rates is stronger than simple reduction in carbon dioxide partial pressure, is seen in the change of reaction rate with weight of carbon charge. A 100% increase in weight of carbon resulted in only a 30% increase in weight of carbon reacting per unit time per unit concentration of carbon dioxide in the bed. This is akin to the results discussed above[1] for the gas-baked carbon rod.

There are some conflicting data, however, regarding the postulate that the reaction is being inhibited by carbon monoxide formation. Doubling the volume flow rate of carbon dioxide through the reactor had a negligible effect on the reaction rate despite the decrease in percentage of carbon monoxide in the reactor. The small change in reaction rate which did occur can be explained as a partial pressure effect. Further, calculations in the Appendix indicate that for the carbon dioxide flow rates used there is some back mixing of carbon monoxide in the reactor. Consequently, an increase in flow rate of carbon dioxide through the reactor should decrease the extent of back mixing and result in an increase in carbon reactivity. A complete understanding of why the reaction rates for the particle carbons are consistently lower than the rates for the rod counterparts must await such experiments as the introduction of varying amounts of carbon monoxide into the entering carbon dioxide stream.

Considering the reaction rate results on the various carbons, it is seen that there is no correlation between reactivity and specific surface area of the carbon. This is simply confirmation of results reported previously by this laboratory.[1, 5, 13] Furthermore, there is no correlation

between crystallinity of the carbons, as given by crystallite size and interlayer spacing, and reactivity. Some of the highly graphitized samples, having large crystallite sizes and small interlayer spacings, react appreciably more rapidly than do their turbostratic carbon counterparts. This fact has also been reported previously for the reaction of rod samples with carbon dioxide.[5] There is likewise no correlation between electrical resistivity of the particle carbons and their reactivity to carbon dioxide. For example, 2750 GC 'B', which has the same electrical resistivity as 3000 Spec under a pressure of 2500 p.s.i., has a reactivity four times that of 3000 Spec. There is no apparent relationship between the amount or nature of the ash in the carbons and their reactivity. Contrary to expectations, both 950 PPC and 950 CTPC have appreciably smaller reactivities to carbon dioxide than their 2750°-counterparts, despite having larger percentages of ash for all substances reported.

A similar lack of correlation between the above physical properties and reactivity of different carbon rods to carbon dioxide was previously pointed out.[5] Only recently has a good qualititive correlation of reactivity results been found. Walker and co-workers[13] correlated the reactivity of moulded, graphitized carbon plates (the filler material being from 12 different sources) to carbon dioxide by determining the relative amount of basal plane and edge carbon atoms exposed in the surface of the plates. The higher the percentage of basal plane carbon atoms in the surface of the plate the lower was the reactivity of the plate to carbon dioxide. The intensity of the (002) X-ray diffraction peak was used as a measure of the relative tendency of the basal planes to orient in the surface of the moulded plates. The greater the intensity of this peak the greater is the tendency for basal plane orientation on moulding. It is now planned to attempt to correlate the reactivities of particle carbons with the intensity of the (002) X-ray diffraction peak. The greater the intensity of this peak, the more unsymmetrical the particle shape should be and the larger the percentage of the particle surface composed of basal plane carbon. The only exceptions found to this correlation, at the moment, are graphitized carbon blacks, where, as shown by Smith & Polley[26] the particle surface is composed solely of basal plane structure presented by pentagonal and hexagonal faces. Here the intensity of the (002) X-ray diffraction peak and the gas reactivity are both at a minimum. A tentative explanation for the reactivities of the two coked pitches being considerably lower than their graphitized counterparts, in the present work, could be that they have a higher percentage of basal plane carbon in their surface, but the proof of this speculation awaits further work.

Summary

(1) A ceramic holder in which the reactivity of particle carbons with carbon dioxide can be determined as a function of burn-off has been described.

(2) Reactivities of carbon rods as previously determined, and their ground counterparts as determined in the present reactor, are found to be in the same relative order, if the particle size of the filler material is essentially similar.

(3) For material with small particle size, such as lampblack, the relative reactivities of particle samples are higher than when reacted in rod form.

(4) The reactivities of all the comparable samples are found to be less in the particle reactor than when reacted in rod form.

(5) It is suggested that carbon monoxide inhibition is responsible for this decrease in reactivity but certain evidence exists to conflict with this interpretation, which must be clarified by further experiments.

APPENDIX

Partition of gas flow between reactor and annulus

In order to interpret the reactivity results, it is necessary to calculate the percentage of the total carbon dioxide flow which enters the reactor under different operating conditions. Once this information is available and having the reactivity data, the percentage conversion of carbon dioxide to carbon monoxide by gasification of the carbon can be calculated. This percentage conversion can be compared with equilibrium data to determine whether attainment of equilibrium is limiting the reactivity of the carbon.

The method of calculation of partition of gas flow between reactor and annular space around the reactor is demonstrated for one set of operating conditions. The equations for isothermal streamline (streamline flow through the reactor and annulus have been verified by Reynold's number calculations) flow necessary to calculate the partition of the carbon dioxide stream are:

(*a*) through straight, circular pipe[27]

$$\frac{dP}{dL} = \frac{4\rho(16/Re)\,V^2}{2gD} = \frac{32\mu V}{gD^2}$$

(*b*) through annular space[27]

$$\frac{dP}{dL} = \frac{32\mu V}{g\left[D_2^2 + D_1^2 - \dfrac{(D_2^2 - D_1^2)}{\ln D_2/D_1}\right]}$$

(*c*) through packed bed[28]

$$\frac{dP}{dL} = \frac{150(1-\varepsilon)^2}{g\varepsilon^3} \cdot \frac{\mu V}{D_p^2}$$

where

A = area
D = diameter, as of the reactor
D_p = effective particle diameter
g = acceleration due to gravity
dL = differential length
dP = differential frictional pressure drop
V = linear gas velocity, equal to volume flow rate, U, divided by cross-sectional area
ρ = density of gas
μ = absolute viscosity of gas
ε = fractional void volume in packed bed, assumed = 0·5

and subscripts:

a   is for gas flow through annulus
r   is for gas flow through reactor
t   is for total gas flow
1   refers to minor diameter of annulus
2   refers to major diameter of annulus

The dimension of the reactor, furnace tube, chips, and carbon charge are taken as follows:
i.d. of reactor = 1·98 cm.
o.d. of reactor = 2·30 cm.
i.d. of furnace tube = 2·90 cm.
diam. of holes (16) in bottom of reactor = 0·22 cm.
total reactor height = 4·72 cm.
effective diam. of 6 × 8 mesh particles = 0·28 cm.
effective diam. of 8 × 20 mesh particles = 0·16 cm.
specific height of 6 × 8 mesh porcelain chips in reactor = 0·27 cm./g.
specific height of 8 × 20 mesh porcelain chips in reactor = 0·25 cm./g.
specific height of 6 × 8 mesh carbon particles in reactor = 0·45 cm./g.

Two g. of 6 × 8-mesh porcelain chips were always used; 8 × 20-mesh chips were added to make a total of 4, 6, or 8 g. of chips, as desired.

The flow partition will be calculated for CO_2 at 1100°, where 6 g. of chips and 2 g. of 950 GBC ' B ' are used. Taking for the carbon dioxide properties

μ = 4·90 × 10^{-5} lb./ft. sec.
ρ = 0·0241 lb./cu. ft.
U_t = 6·04 × 10^{-3} cu. ft./sec.

and using the equations presented above, the various pressure drops are calculated as:

1. Through annulus $\Delta P_a = 0\cdot0676 - 11\cdot2\ U_r$

2. Through reactor bottom $\Delta P_{r-1} = 7\cdot5\ U_r$

3. Through 6–8-mesh porcelain chips $\Delta P_{r-2} = 28\cdot5\ U_r$

4. Through 8–20-mesh porcelain chips $\Delta P_{r-3} = 161\ U_r$

5. Through 6–8-mesh carbon particles $\Delta P_{r-4} = 47\cdot2\ U_r$

and equating pressure drops to find U_r, $\Delta P_a = \Delta P_{r-1} + \Delta P_{r-2} + \Delta P_{r-3} + \Delta P_{r-4}$

or

$$U_r = 0\cdot000265\ \text{cu. ft./sec.}$$

From this calculation, the percentage of the total carbon dioxide flow entering the reactor is 4·4%, and the percentage of carbon monoxide in the mixture leaving the reactor is 25·0%, taking the reaction rate for the 950 GBC ' B ' at 1100° as 0·41 g./h. It is understood that because of the formation of two moles of carbon monoxide for each mole of carbon dioxide reacting and the resulting increase in pressure drop, the amount of carbon dioxide entering the reactor would be less than that calculated. The percentage decrease in the calculated amount of carbon dioxide entering the reactor would be less than the percentage of carbon monoxide formed (since all the carbon monoxide formed does not increase the pressure drop along the full length of the reactor), and such a correction would not alter the conclusions which will be made on the basis of these calculations. Table IX presents data for the calculated percentage of carbon monoxide leaving the reactor for various operating conditions.

Table IX

Tabulated percentages of CO in reactor for various operating conditions

Condition*	Carbon	% of total CO$_2$ going to reactor	Reaction rate (g./h.)	% CO in CO–CO$_2$ mixture leaving reactor
2-2-2-1100-2200	2750 GC ' B '	6·4	0·22	10
2-4-2-1100-2200	2750 GC ' B '	4·4	0·20	13
2-6-2-1100-2200	2750 GC ' B '	3·3	0·20	17
2-4-2-1100-2200	950 GBC ' B '	4·4	0·41	25
2-4-3-1100-2200	950 GBC ' B '	4·0	0·47	30
2-4-4-1100-2200	950 GBC ' B '	3·7	0·53	36
2-4-2-1130-1450	2750 GC ' B '	4·3	0·28	26
2-4-2-1130-2200	2750 GC ' B '	4·3	0·30	19
2-4-2-1130-2850	2750 GC ' B '	4·3	0·30	15

*In order: wt. 6 × 8-mesh porcelain, 8 × 20-mesh porcelain, 6–8-mesh carbon; temp., °c; flow in c.c./min.

Extent of back mixing in the reactor

Ergun[29] has shown the marked effects which back mixing of the reaction products can have on the rate of the carbon–carbon dioxide reaction in a fixed bed. For sufficiently high, constant flow-rates of carbon dioxide, the introduction of helium into the gas stream does not change the fraction of carbon dioxide reacting. This is interpreted to mean that there is negligble back mixing at all flow rates. On the other hand, at a low, constant flow-rate of carbon dioxide, the introduction of sufficient helium can actually increase the percentage of carbon dioxide reacting by changing the flow pattern from complete to negligible back mixing. Between these two extremes, there is a transition flow region over which continuous change in helium flow rate

produces an accompanying continuous change in percentage of carbon dioxide reacted. For the reaction conditions discussed in the previous section, the extent of back mixing is approximated as follows:

The diffusion rate at a point is given by

$$N_A = -D\frac{dc}{dx} \quad \text{where:}$$

N_A = diffusion rate in mol./sec./sq. cm. dc = differential concentration in moles/c.c.
D = diffusion coefficient in sq. cm./sec. dx = differential distance in cm.

with the diffusion coefficient, D, for the mixture of carbon monoxide and carbon dioxide at 1100° and atmospheric pressure taken as equal to 7·6 sq. cm./sec. For 2 g. of 950 GBC ' B ' and a carbon dioxide flow-rate of 2200 c.c./min., the concentration of carbon monoxide at the top of the particle bed is approximated as 1·3 μmoles/c.c. Assuming zero concentration of carbon monoxide at the entrance to the bed, N_A × (cross-section of bed, assuming 50% void volume) equals 12·0 μmoles/sec. From the previous section, it was calculated that the total gas flow-rate upward in the bed was 2·65 × 10⁻⁴ cu. ft./sec. or 69·4 μmoles/sec. of which, on an average through the bed, $\sim$ 12·5% is carbon monoxide. Therefore, 8·7 μmoles/sec. of carbon monoxide will flow up through the bed. To balance the flow of carbon monoxide up through the bed with its rate of back diffusion, the concentration of carbon monoxide at the entrance to the bed would equal 0·28 μmole/c.c. This represents about 20% of the carbon monoxide at the top of the bed and indicates that this particular condition is in the transition range between negligible and complete back mixing.

Acknowledgments

References

[1] Walker, P. L., jun., Foresti, R. J., jun., & Wright, C. C., *Industr. Engng Chem.*, 1953, **45**, 1703
[2] Walker, P. L., jun., McKinistry, H. A., & Wright, C. C., *Industr. Engng Chem.*, 1953, **45**, 1711
[3] Walker, P. L., jun., & Wright, C. C., *Industr. Engng Chem.*, 1953, **45**, 1715
[4] Walker, P. L., jun., McKinistry, H. A., & Pustinger, J. V., *Industr. Engng Chem.*, 1954, **46**, 1651
[5] Walker, P. L., jun., & Rusinko, F., jun., *J. phys. Chem.*, 1955, **59**, 241
[6] Walker, P. L., jun., Rusinko, F., jun., & Raats, E., *J. phys. Chem.*, 1955, **59**, 245
[7] Walker, P. L., jun., & Rusinko, F., jun., *Fuel, Lond.*, 1955, **34**, s22
[8] Petersen, E. E., Wright, C. C., & Walker, P. L., jun., *Industr. Engng Chem.*, 1955, **47**, 1629
[9] Walker, P. L., jun., Rusinko, F., jun., & Raats, E., *Nature, Lond.*, 1955, **176**, 1167
[10] Walker, P. L., jun., & Raats, E., *J. phys. Chem.*, 1956, **60**, 364, 370
[11] Walker, P. L., jun., *Proc. Conf. on Carbon, Buffalo, N.Y.*, 1956, pp. 75-81
[12] Walker, P. L., jun., & Rusinko, F., jun., ' Effect of Impregnation and Subsequent Burn-off on Physical Properties of Graphitized Carbon Rods ', 3rd Conf. on Carbon, Buffalo, N.Y., June 17–21, 1957, in press
[13] Walker, P. L., jun., Rusinko, F., jun., Rakszawski, J. F., & Liggett, L. M., ' Effect of Different Cokes on Physical Properties of Graphitized Carbon Plates ', 3rd Conf. on Carbon, Buffalo, N.Y., June 17–21, 1957, in press

[14] Emmett, P. H., *A.S.T.M. Tech. Publ.*, 1941, **51**, 95
[15] Beebe, R. A., Beckwith, J. B., & Honig, J. M., *J. Amer. chem. Soc.*, 1945, **67**, 1834
[16] Walker, P. L., jun., & Rusinko, F., jun., *Fuel, Lond.*, 1957, **36**, 43
[17] ' Methods for Spectrochemical Analysis ', 1953, pp. 19ff, 43 (A.S.T.M.)
[18] A.S.T.M. Standard D271-48, ' Standard Methods of Laboratory Sampling and Analysing Coal and Coke ', *A.S.T.M. Standards*, 1952, **5**, 807
[19] Stanton, F. M., Fieldner, A. C., & Selvig, W. A., ' Methods of Analysing Coal and Coke ', *U.S. Bur. Min.*, 1939, Tech. Paper No. 8
[20] Katz, M. J., *J. phys. Chem.*, 1956, **60**, 1338
[21] Pinnick, H. T., *Proc. Conf. on Carbon, Buffalo, N.Y.*, 1956, p. 3–11
[22] Wicke, E., 5th Symposium on Combustion, Williams & Wilkins Co., Baltimore, Md., 1955, p. 249
[23] Kuchta, J. M., Kant, A., & Damon, G. H., *Industr. Engng Chem.*, 1952, **44**, 1559
[24] Gadsby, J., Long, F. J., Sleightholm, P., & Sykes, K. W., *Proc. roy. Soc.*, 1948, [A] **193**, 357
[25] Ergun, S., *J. phys. Chem.*, 1956, **60**, 480
[26] Smith, W. R., & Polley, M. H., *J. phys. Chem.*, 1956, **60**, 680
[27] McAdams, W. H., ' Heat Transmission ', 1942, chap. 5 (New York: McGraw Hill Book Co.)
[28] Ergun, S., *Chem. Engng Progr.*, 1952, **48**, 88
[29] Ergun, S., *Industr. Engng Chem.*, 1955, **47**, 2075

Discussion

Dr. T. B. Copestake: Dr. Walker may be interested in some results that we have obtained bearing on his investigation into the effect of graphitization temperature on reactivity. We find that heating commercial graphite to about 2500° and cooling in argon reduces its reactivity to carbon dioxide about 1000-fold at 500°. In looking for an explanation of this phenomenon, I think one must recall how graphite is made. It is cooled in an atmosphere that we have shown to contain considerable quantities of carbon dioxide and hence may be oxidizing to the graphite. The surface of the graphite will therefore be corroded and will consist of disordered layers. I believe it is these atoms which are responsible for oxide formation in carbon dioxide and that perhaps the effect of heating to 2500° is to evaporate these atoms leaving well ordered unreactive layers.

Prof. Walker: I could discuss Dr. Copestake's interesting comment at considerable detail, but I feel that several experimental facts indicate that the answer is more complex than he suggests.

(1) In the paper, it is seen that the reactivity of petroleum coke does not increase after graphitization even though it was exposed to the same furnace atmosphere (Acheson furnace) as were the coal-tar pitch coke and petroleum pitch coke, both of which increased markedly in reactivity after graphitization.

(2) The extent of carbon–oxygen surface complex is extremely important in determining the rate of gasification at very low burn-offs. The extent of this initial complex does not, however, significantly affect gasification rates at intermediate and high burn-offs.

(3) In some recent work, six coal-tar pitch cokes and a delayed petroleum coke were graphitized and cooled in a helium atmosphere. The coal-tar pitch cokes all showed a marked increase in reactivity to carbon dioxide after graphitization (a similar finding to that in the present paper). The petroleum coke showed a marked decrease in reactivity after graphitization. There, therefore, appears to be a basic difference in the effect of heat-treatment on cokes, depending upon whether the coke is produced from a material which has been volatilized from the source material (coal-tar pitch coke or petroleum pitch coke) or is produced from the residue of the source material (delayed petroleum coke, for example). It is thought that the difference is connected with the degree of association of the impurities with the carbon matrix and the effect of temperature on this association. Extensive research is in progress on this point.